Characterization of a New Microporous Lithozincosilicate with ANA Topology

So-Hyun Park,† Hermann Gies,‡ Brian H. Toby,§ and John B. Parise*,†,||

Department of Geosciences, State University of New York at Stony Brook, New York 11794-2100, Institut für Geologie, Mineralogie, Geophysik, Ruhr-Universität-Bochum, 44801 Bochum, Germany, NIST Center for Neutron Research, National Institute of Standards and Technology, Gaithersburg, Maryland 20899-8562, and Department of Chemistry, State University of New York at Stony Brook, New York 11794-2100

Received March 4, 2002. Revised Manuscript Received May 6, 2002

A new microporous lithozincosilicate ($Cs_{12}Li_{13}[Li_3Zn_8Si_{37}O_{96}]\cdot 4H_2O$), an analogue of pollucite ($CsAlSi_2O_6$) and analcime ($NaAlSi_2O_6$), contains lithium in both framework and nonframework sites. This represents the first example of the incorporation of lithium into the ANA framework structure type. The analysis of the crystal structure used X-ray and neutron powder diffraction techniques, which reveal partially ordered sites in the framework occupied by Li, Zn, and Si atoms. The framework sites are occupied in a manner to distribute the low valent cations as far apart as possible. The pore system of the material consists of large cuboctahedra, occupied by Cs and water molecules, and smaller vacancies available for siting of nonframework Li bounded by six- and eight-membered rings of framework tetrahedra.

Introduction

The naturally occurring aluminosilicate pollucite ($Cs[AlSi_2O_6]\cdot xH_2O$) possesses an open framework composed of corner-sharing TO_4 units.[1] Here, T refers to the tetrahedrally coordinated sites randomly occupied by Al^{3+} and Si^{4+}. The TO_4 units are connected to form four- and six-membered rings (MR) that interconnect via additional oxygen bridges to build a four-connected three-dimesional network (Figure 1). The structure contains a three-dimensional channel system with distorted 8MR openings. Additionally, there are large cavities occluding Cs^+ cations or water molecules, bounded by 12 framework oxygens, as well as octahedral vacancies available for smaller cations such as Na^+ and Ag^+.[2] The topology of the pollucite structure has the International Zeolite Association (IZA) structure type ANA[3] originating from the name and topology of a mineral analcime ($Na[AlSi_2O_6]\cdot H_2O$).[4] The mineral leucite ($K[AlSi_2]O_6$)[5] and synthetic compounds such as members of the $M_2[TSi_5O_{12}]$ family (M = Cs, Rb, K, Na; T = Be, Mg, Fe, Co, Ni, Zn, Cd, B, Ga, Ge)[6] also crystallize in the ANA structure type. Typically, ANA-type materials are thermally stable and readily incorporate penta-, tetra-, tri-, and divalent cations in the framework T sites.

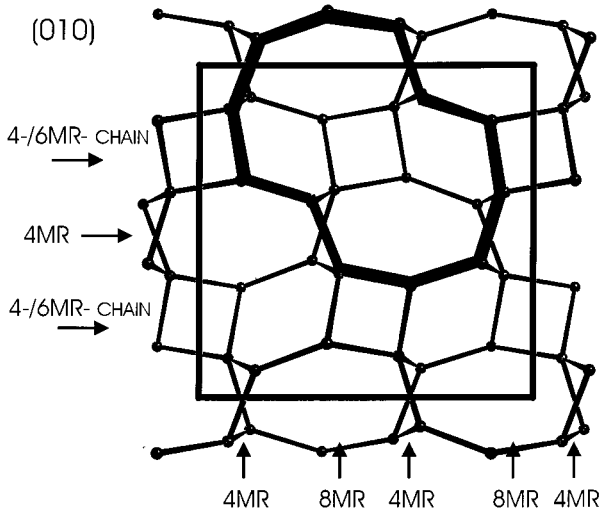

Figure 1. Projection of the pollucite framework structure on (010). 4MR/6MR chains are connected via 4MRs in the three-dimensional space. The highlighted boldfaced line presents the skirt line of two attached cuboctahedral pore voids. The centers of framework tetrahedra (small circles) are indicated.

Despite the presence of large cuboctahedral pore voids (Figure 1), access to them is restricted through distorted channel openings, and ANA-type materials have a low

* To whom correspondence should be addressed. Phone: +1 (631) 632 8196. Fax: +1 (631) 632 8140. E-mail: jparise@notes.cc.sunysb.edu or sohpark@notes.cc.sunysb.edu.

† Department of Geosciences, State University of New York at Stony Brook.

‡ Institut für Geologie, Mineralogie, Geophysik, Ruhr-Universität-Bochum.

§ National Institute of Standards and Technology.

|| Department of Chemistry, State University of New York at Stony Brook.

(1) Náray-Szabó, St. *Z. Kristallogr.* **1938**, *99*, 277.
(2) Beger, R. M. *Z. Kristallogr.* **1969**, *129*, 280.
(3) See references for *Isotypic framework structures of ANA-type, Atlas of Zeolite framework types,* 5th revised ed.; Baerlocher, Ch., Meier, W. M., Olson, D. H., Eds.; Elsevier: New York, 2001.
(4) Taylor, W. H. *Z. Kristallogr.* **1930**, *74*, 1.
(5) Peacor, D. R. *Z. Kristallogr.* **1968**, *127*, 213.
(6) Torres-Martinez, L. M.; West, A. R. *Z. Kristallogr.* **1986**, *175*, 1.

10.1021/cm020226w CCC: $22.00
Published on Web 06/12/2002

ion-exchange capability. Once exchanged, however, this restricted access suggests that ANA frameworks may be useful for the sequestration of radioactive Cs or Sr. For example, McCready et al.[7] investigated a new synthetic pollucite analogue, $CsTiSi_2O_{6.5}$, and discussed its potential application for the treatment of radioactive Cs-loaded nuclear wastes incorporating high concentrations of Ti-bearing compounds. For this application, it is desirable to tailor the ion-exchange capacity so as to produce a composition suitable for sintering to stable nonexchangeable dense phases[8] or to maximize the number of cations exchanged into the pores. Such control is readily achieved in the compositionally flexible ANA-type materials, by substituting low valent atoms such as Be^{2+}, Mg^{2+}, and Zn^{2+} at the T sites. The greatest number of nonframework charge balancing cations per T site substitution is achieved through replacement of Si^{4+} with Li^+. Prior to this work, this substitution remained unknown. We describe here a new ANA family member related to pollucite, $Cs_{12}Li_{13}[Li_3Zn_8Si_{37}O_{96}]\cdot 4H_2O$, in which monovalent Li^+ cations are incorporated along with Zn^{2+} into the $[SiO_4]$ network.

Experimental Section

Synthesis of the Microporous Material. The microporous lithozincosilicate (Lab-Code RUB-31: Ruhr-Universität-Bochum, number 31) was initially found as a byproduct from a reaction mixture of the molar composition 1 SiO_2/0.03 ZnO/0.23 Li_2O/0.23 Cs_2O/0.08 TEAOH/44 H_2O[9] in the synthesis of two new lithosilicates RUB-23 ($Cs_{10}(LiH)_{14}[Li_8Si_{40}O_{96}]\cdot 12H_2O$)[10] and RUB-29 ($Cs_{14}Li_{24}[Li_{18}Si_{72}O_{172}]\cdot 14H_2O$).[11] To maximize the yield of RUB-31 crystals, the amount of zinc in the gel was increased by a factor of 3, and the synthesis was conducted in rotating reaction vessels. A typical synthesis mixture producing RUB-31 was prepared as follows: 4.09 mL of tetraethylammonium hydroxide (TEAOH, 35% in water, Aldrich), 11.38 mL of cesium hydroxide (50% in water, Aldrich), and 2.74 g of $LiOH\cdot H_2O$ (Fisher) were added to 100 mL of deionized water. With vigorous stirring, 1.16 g of ZnO (99%, Fluka) was added bit-by-bit into the solution, and then 21.04 mL of the silica source, tetramethoxysilane (TMOS, >98%, Aldrich), was added dropwise over 3 h. After agitation for another 2 h, the resulting reaction mixture was charged into four Teflon-lined stainless steel autoclaves with a capacity of 50 mL and allowed to react at 190 °C under rotating conditions for 2 weeks. The product was washed several times with distilled water and ethanol and dried at room-temperature overnight. Typically, about 2 g of crystalline RUB-31 was produced from each reaction vessel.

Physico-Chemical Analysis. The chemical components silicon, zinc, and cesium of as-synthesized RUB-31 material were analyzed using an electron micro probe (EMP; Camera SX50), and lithium and the total water content were determined by atomic absorption spectrophotometry (AAS; Perkin-Elmer 4000) and the Karl−Fisher method, respectively. For characterization of optical properties under polarized light, samples embedded in epoxy, polished, and mounted on a thin glass plate were observed using a Zeiss microscope. Details of the crystal morphology were determined using a scanning electron microscope (Stereoscan 250, MK3D); a typical photograph is shown in Graph 1.

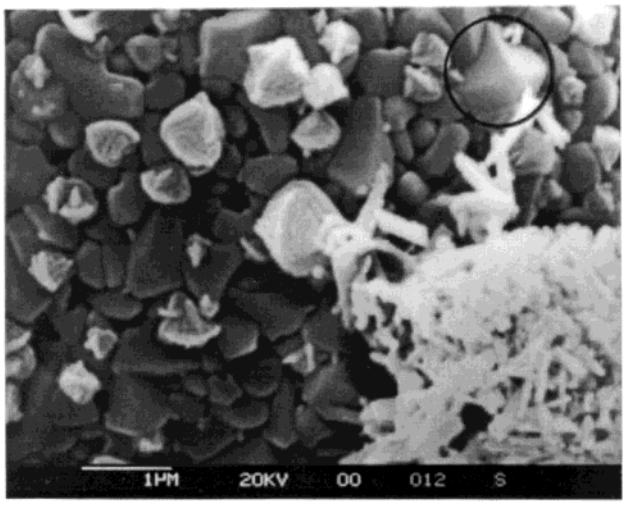

(**Graph 1.** Scanning electron micrograph of RUB-31 crystal aggregate. A well-formed individual RUB-31 crystal is emphasized with a circle (right side of the top). The graph also shows that the RUB-31 aggregate surface is partially contaminated by another aggregate of Li_2SiO_3 and Zn_2SiO_4 (right side of the bottom)).

Solid-state nuclear magnetic resonance (NMR) spectroscopy was performed with the as-synthesized material on a Bruker ASX 400 spectrometer. Magic-angle spinning (MAS) spectra were recorded using spinning speeds of 3.5, 10, and 5 kHz for ^{29}Si, ^{7}Li, and ^{133}Cs NMR, respectively. To acquire ^{29}Si spectra, a pulse width of 5 μs ($\pi/2$ pulse) with a recycle time 120 s were applied. ^{7}Li MAS NMR spectra were measured with a pulse width of 0.6 μs ($\pi/24$ pulse) and recycling delays of 1 s. To obtain ^{133}Cs spectra, a pulse width of 0.5 μs ($\pi/24$ pulse) and recycle delays of 1 s were applied. Tetramethylsilane (TMS), a 1 M LiOH solution, and a 1 M CsOH solution were used to refer ^{29}Si, ^{7}Li, and ^{133}Cs NMR, respectively, at 0 ppm.

Powder X-ray diffraction (XRD) data of as-synthesized RUB-31 sample were collected on a Siemens D5000 diffractometer with Debye−Scherrer geometry (Cu $K\alpha_1$ radiation, $\lambda = 1.5406$ Å). In a 2θ range between 5° and 95°, the measurement was repeated 4 times with a step size of 0.007 766° (2θ) where the instrumental resolution was a peak half-width of 0.06 °(2θ). These four data sets were merged to increase the signal-to-noise discrimination for subsequent structure analysis.

To obtain neutron powder diffraction (NPD) data of the dehydrated RUB-31 material, 1 g of as-synthesized sample was treated at 200 °C in a vacuum for 5 h and rehydrated with D_2O. This D_2O-exchanged sample was again dehydrated at 200 °C overnight. This entire dehydration procedure was repeated twice more before the sample was sealed into a vanadium can within a glovebox. NPD data were collected using the 32 detector BT-1 neutron powder diffractometer at the NIST NBSR reactor in Gaithersburg, MD. Measurements were conducted under ambient conditions using a Ge(311) monochromator with a wavelength $\lambda = 2.0783(2)$ Å.

The behavior of RUB-31 at high temperature was characterized by in situ dehydration experiments. An as-synthesized sample was loaded into a silica capillary with a diameter of 1 mm. The sample was then continually heated at 10 °C/min from room temperature (RT) up to 800 °C and then quenched to RT. Structural changes were monitored with an image-plate detector (MAR345) using time-resolved synchrotron X-ray powder diffraction techniques ($\lambda = 0.9274$ Å) at the beam line X7B in National Synchrotron Light Source at Brookhaven National Laboratory, NY.

Structure Analysis. The X-ray powder diffraction (XPD) data were indexed using the program TREOR90.[12] A prelimi-

(7) McCready, D. E.; Balmer, M.-L.; Keefer, K. D. *Powder Diffr.* **1997**, *12* (1), 40.

(8) Nyman, M.; Tripathi, A.; Parise, J. B.; Maxwell, R. S.; Harrison, W. T. A.; Nenoff, T. M. *J. Am. Chem. Soc.* **2001**, *123*, 1529.

(9) Park, S.-H. Ph.D. Thesis, Ruhr-Universität, Bochum, Germany, 1998.

(10) Park, S.-H.; Daniels, P.; Gies, H. *Microporous Mesoporous Mater.* **2000**, *37*, 129.

(11) (a) Park, S.-H.; Parise, J. B.; Gies, H.; Liu, H.; Grey, C. P.; Toby, B. H. *J. Am. Chem. Soc.* **2000**, *122*, 44, 11023; (b) Park, S.-H.; Parise, J. B.; Gies, H. *Proceedings of the 13th International Zeolite Conferences*, Montpellier, France, 8−13 July 2001.

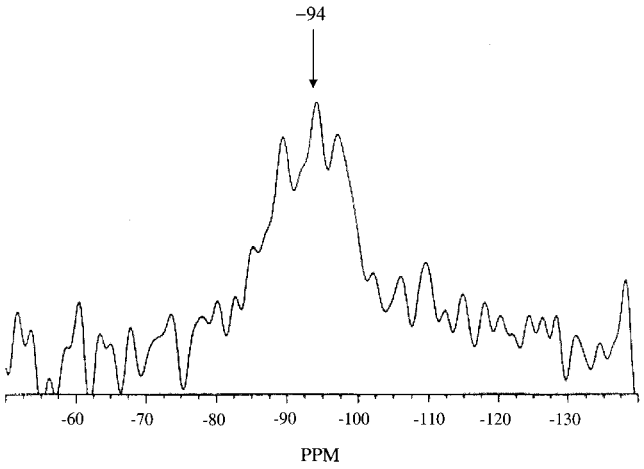

Figure 2. ^{29}Si MAS NMR spectrum of as-synthesized RUB-31. A broad resonance at about −94 ppm displays a splitting of three fine peaks (see text).

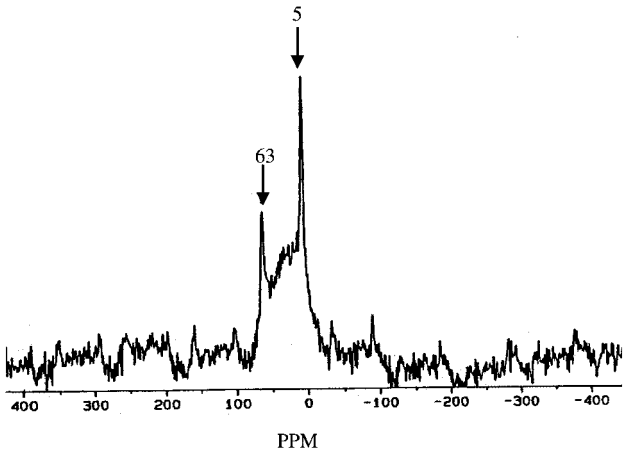

Figure 3. ^{133}Cs MAS NMR spectrum of as-synthesized RUB-31. Two sharp resonances with different intensities indicate at least two distinguishable surroundings for Cs cations with different amounts in the RUB-31 pore system.

nary structure model was derived from the pollucite structure[1] and refined using a combination of distance least-squares (DLS) calculations and Rietveld analysis with DLS-76[13] and XRS-82,[14] respectively. To confirm the framework model thus obtained, and to better determine the sites occupied by lithium cations, NPD data were analyzed using the implementation of Rietveld analysis in the GSAS[15] suite.

Results and Discussion

Chemical and Optical Properties. EMP and AAS analysis results are consistent with a ratio of 1.9(1) Cs/1.0(2) Zn/2.6(6) Li/4.7(2) Si/1.0(2) H_2O for the bulk composition of as-synthesized RUB-31 sample. Polarized light microscopy indicates that RUB-31 crystallizes in spherical aggregates that are optically isotropic, indicating cubic symmetry. The scanning electron micrographs (Graph 1) showed that individual RUB-31 crystals are less than 1 μm in size and are partially coated with fine needle-shaped impurity phases.

^{29}Si, ^{133}Cs, and ^{7}Li MAS NMR Spectroscopy. The ^{29}Si MAS NMR spectrum (Figure 2) displays a broad resonance at −94 ppm. On the basis of ^{29}Si MAS NMR spectra of microporous zincosilicates[16] and lithosilicates,[10,11] the chemical shift at −94 ppm in the ^{29}Si NMR spectrum of RUB-31 indicates isomorphic replacements of framework silicon atoms by zinc or lithium. Interestingly, the ^{29}Si NMR resonance shows a fine structure, being resolved into three peaks. This suggests silicon atoms located on at least three distinct sites.

Two distinct resonances at about 5 and 63 ppm are observed in the ^{133}Cs MAS NMR spectrum (Figure 3). These indicate at least two different surroundings for Cs cations within the RUB-31 pore system, and their intensity ratio is proportional to their occupancy.[17] Therefore, the ^{133}Cs NMR resonance at 5 ppm might be due to a higher population of Cs cations at one site within the pore system of RUB-31 than those associated with the resonance at about 63 ppm (Figure 3). The ^{7}Li MAS NMR spectrum of RUB-31 contains a very broad resonance with a shoulder in the high-filed side (Figure 4). This shoulder could be due to several symmetrical unique Li sites within RUB-31 or the presence of Li-bearing impurity phases in the sample, as shown in the structure analysis with NPD data (see the following sections).

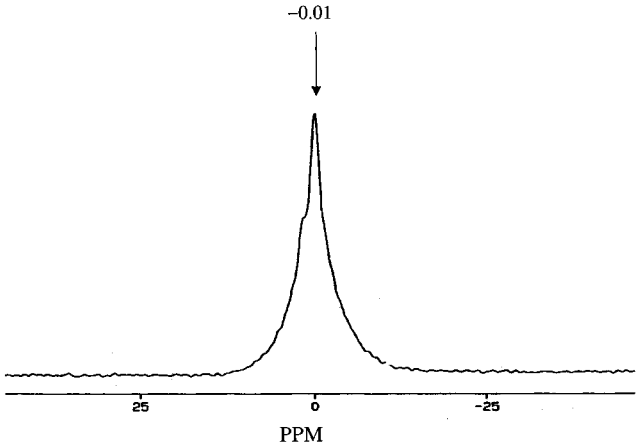

Figure 4. ^{7}Li MAS NMR spectrum containing a strong broad resonance at 0 ppm. The shoulder in the left side of the peak can be due to Li-bearing impurity in the sample or several symmetrically unique Li positions in the RUB-31 structure.

Indexing and Phase Identification. All observed XPD reflections could be indexed on the basis of a primitive cubic cell with reflections violating the ideal body centered symmetry of the ANA structure type, such as (410), (430), (540), and (630), clearly visible (Figure 5). There was also no indication of lower symmetry or of the impurity phases found in the SEM (Graph 1). Impurities later identified as Li_2SiO_3 and Zn_2-

(12) Werner, P. E.; Erikson, L.; Westdahl, M. TREOR, A semiexhaustive trial-and-error powder indexing program for all symmetries. *J. App. Crystallogr.* **1985**, *18*, 367.

(13) Baerlocher, Ch.; Hepp, A.; Meier, W. M. *DLS-76, A program for the simulation of crystal structures by geometric refinement*; Institut für Kristallographie: ETH, Zürich, Switzerland, 1977.

(14) Baerlocher, Ch. *XRS-82, The X-ray Rietveld System (Unix-Version)*; Institut für Kristallographie: ETH, Zürich, Switzerland, 1991.

(15) Larson, A. C.; Von Dreele, R. B. *GSAS, General Structure Analysis System*; LANSCE, MS-H805; Los Alamos National Laboratory, Los Alamos, NM, 1986.

(16) (a) Annen, M. J.; Davis, M. E. *Microporous Mater.* **1993**, *1*, 57. (b) Röhrig, C.; Dierdorf, I.; Gies, H. *J. Phys. Chem. Solids* **1995**, *56* (10), 1369. (c) Camblor, M. A.; Davis, M. E. *J. Phys. Chem.* **1994**, *98*, 13151.

(17) Koller, H.; Burger, B.; Schneider, A. M.; Engelhardt, G.; Weitkamp, J. *Microporous Mater.* **1995**, *5*, 219.

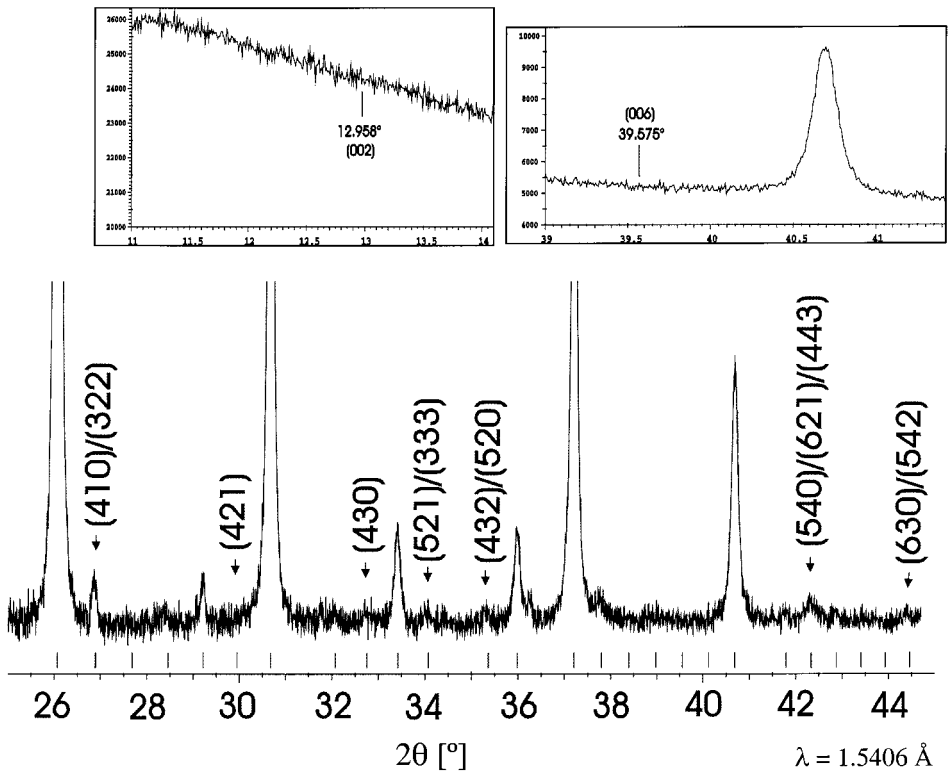

Figure 5. Part of indexed observed XPD profile of as-synthesized RUB-31 after background correction (bottom). The bars marked on the bottom correspond to all possible reflections for RUB-31, and superstructure reflections of primitive cubic lattice ($P4_132$) are extra given with their Miller's indices which cannot be indexed in the body-centered cubic cell of pollucite ($CsAlSi_2O_6$). Two embedded diagrams (above) were obtained from the observed XPD data of as-synthesized RUB-31 without any data reduction in the range of 11−15° (2θ) and 39−42° (2θ), respectively. The XPD diagrams clearly show the absence of the reflection (002) and (006), by which the space group symmetry $P2_13$ could be excluded as a possible candidate for the RUB-31 symmetry.

SiO_4 were more obvious in the NPD data, possibly indicative of the greater penetrating power of neutron radiation. The space group symmetry of RUB-31, $P4_132$, is one of the primitive cubic subgroups of $Ia\bar{3}d$. Another possible cubic subgroup $P2_13$ could be excluded due to the absence of (00l) with $l = 2n$ like (002) and (006) in XPD pattern (Figure 5). The tetragonal primitive symmetry $P4_12_12$ was also not considered based upon the optically isotropic behavior of RUB-31 under polarized light.

Structure Analysis. Rietveld calculations using the XPD data proceeded on the basis of chemical analysis results. Because of their relative sensitivity to lithium, the structure refinement of RUB-31 has been completed using NPD data. Rietveld analysis using XPD data, however, confirmed the symmetry of the structure containing the new combination of framework cations.

First Step: *Derivation of a Structure Model of RUB-31 by DLS and Rietveld Calculations with XPD Data.* To fit the observed XPD profile, zero point, cell parameters, and peak-form functions were determined by analyzing a standard peak at $2\theta_{(321)} = 24.363°$. This standard peak is decomposed into a symmetric and an asymmetric part.[14] These output functions could then be applied in the whole-profile fitting structure refinement as a function of 2θ.

Rietveld refinements were carried out with a starting model that was primarily derived from the pollucite structure, $CsAlSi_2O_6$,[1] corresponding to space group symmetry $P4_132$; for example, one general site T1 and two special sites T2 and T22 for RUB-31 are generated from one general position T of the pollucite structure

Table 1. Symmetrical Unique Si, O, and Cs Sites of RUB-31, Derived from Pollucite[a]

pollucite, $Ia\bar{3}d$[1]	site	RUB-31, $P4_132$	site
T (Si, Al)	48f	T1 (Si)	24e
		T2 (Si)	12d
		T22 (Si)	12d
O	96h	O1	24e
		O12	24e
		O2	24e
		O22	24e
Cs	16b	Cs1	8c
		Cs2	4b
		Cs3	4a

[a] For simplifying the starting model, only Si is considered as framework cations siting on T1, T2, and T22.

(Table 1). On the basis of this model in combination with the chemical analysis results, an idealized structure formula, $Cs_{16}Li_{16}Zn_8Si_{36}O_{96}\cdot(H_2O)_8$, was obtained ($Z = 8$). DLS calculations were performed to optimize the framework part of the model with the refined unit cell parameter $a = 13.6526(1)$ Å. On the basis of the structural data of $CsAlSi_2O_6$, geometrical restrains were given in the DLS calculations: $d(T-O) = 1.64 \pm 0.01$ Å, $\angle(T-O-T) = 145° \pm 8°$, and $\angle(O-T-O) = 109° \pm 4°$.

The resulting atomic coordinates were refined by Rietveld analysis. With isotropic displacement parameters for Cs sites constrained to be equal, refinement of positional and displacement parameters for Cs sites alone resulted a discrepancy index $R_{wp} = [\Sigma w_i(Y_{io} - Y_{ic})^2/\Sigma w_i Y_{io}2]^{0.5}$ of 0.164; here, Y_{io} and Y_{ic} indicate the observed and calculated intensities, respectively, at step i, and the weighting factor $w_i = 1/\sigma(Y_{io})$. Subsequent

Table 2. Comparison of Dimension of Electron Density from Fourier Synthesis on Each Tetrahedral T Site to the Calculated Occupancy Based on the Structure Unit Content from Chemical Analysis, Relating to 100% Occupation of Si for All T Sites[a]

tetrahedral site/ multiplicity	dimension of Fourier peak	ratio of each Fourier peak density relating to the value at T2	estimated occupancy value
T1/24	387	1.56	$1.38 = (8N_{e[Zn]} + 16N_{e[Si]})/24N_{e[Si]}$
T2/12	247	1	$1 = (12N_{e[Si]})/12N_{e[Si]}$
T22/12	195	0.79	$0.74 = (4N_{e[Li]} + 8N_{e[Si]})/12N_{e[Si]}$

[a] $N_{e[atom]}$: number of electrons of [atom].

refinements relaxed constraints on interatomic distances for framework sites, which were $d(T-O) = 1.64 \pm 0.10$ Å, and these clearly showed a distinction between the three tetrahedral sites T1, T2, and T22 with respect to their respective mean values of $d_m(T-O)$ distances. Specifically, the $d_m(T1-O) = 1.76$ Å and $d_m(T2-O) = 1.64$ Å distances are much larger than $d_m(T22-O) = 1.44$ Å. Accordingly, the framework was further optimized by DLS with new restraints on distance values and weights: $d(T1-O) = d(T22-O) = 1.70 \pm 0.05$ Å and $d(T2-O) = 1.60 \pm 0.05$ Å.

The resulting atomic coordinates for the framework constituents provided input for the next cycles of Rietveld analysis, carried on to determine the constrained isotropic displacement parameters for the T1, T2, and T22 sites; one value was refined for all three sites, resulting in U_{iso}, = 0.012(2) (Å^2). Subsequently, occupation factors for these tetrahedral sites were refined, assuming initially that they were occupied only by Si; all displacement parameters and occupation factors for Cs sites were fixed at 100%. The T2 occupancy is 1, indicating that this site is fully occupied by silicon. The ratio of occupancies for the T1, T2, and T22 sites are 1.56:1:0.79 (Table 2), suggesting that the T1 site can be occupied only by silicon and heavier atoms and, in this case, zinc is the only candidate species. Further, the T22 site is occupied by Si and lighter species, such as lithium or vacancies. Interatomic distances for 4-fold coordinated Si, Zn, and Li in silicate materials[18] indicate that $d_m(Zn-O) \approx d_m(Li-O) = 1.96$ Å are much longer than $d_m(Si-O) = 1.60$ Å. The $d_m(T22-O)$ distance in RUB-31 is longer than $d_m(T2-O)$, indicating that silicon atoms on this site are partially substituted by Li rather than occupied by vacancies.

All eight zinc atoms of the structure formula of RUB-31 would then occupy the T1 site (multiplicity $M = 24$) along with 16 Si atoms, resulting in an occupancy value of 1.38 for T1 (Table 2). As mentioned previously, the special position T2 ($M = 12$) should be occupied only by 12 Si atoms, which corresponds to an occupancy of 1. The chemical analysis resulted in 36 silicon atoms per one RUB-31 unit cell. Among them, only eight Si atoms remain available for occupying another special site, T22, as 16 Si atoms along with eight Zn occupy the T1 site and the other 12 Si atoms are siting on the T2 site. Considering this, the T22 site, with a multiplicity of 12, would be occupied by eight Si atoms with four Li atoms. As a result, an occupancy value of 0.74 could be calculated for the T1 site. The resulting ratio of occupancies for the T1, T2, and T22 sites are 1.38:1:0.74, which is close to the value estimated with their Fourier electron densities (Table 2).

The last cycle of Rietveld calculations was performed to refine the positions of partially ordered T sites with their revised occupations, T1(16Si + 8Zn), T2(12Si), and T22(8Si + 4Li), which resulted in an improved discrepancy indices $R_{wp} = 0.154$. The structure analysis with XPD suggested a new pollucite framework structure model with partially ordered [(Si, Zn)O_4], [SiO_4], and [(Si, Li)O_4] tetrahedra on the T1, T2, and T22 site, respectively. The degree of agreement of this model with observed XPD profile is graphically presented in Figure 6. Experimental parameters in collection of the XPD data, geometrical restrains used in Rietveld calculations, and the final refined structure model are summarized in Table 3.

Given the dominance of X-ray scattering from Cs, the locations of nonframework lithium and water positions could not be determined reliably using Rietveld calculations with the XPD data alone. We suspected that lithium occupies octahedral sites in the RUB-31 structure while, like for Cs cations, the only available spaces for water molecules are in the large cuboctahedra cages. This possible partial occupation of water molecules on Cs sites cannot be confirmed by Rietveld analysis with XPD data because of a strong correlation of occupation factors of heavy Cs atoms with the scale factor of the XPD profile. To more reliable determine crystallographic parameters of lithium and cesium cations, we carried out further structure refinements using NPD data collected on dehydrated RUB-31.

Second Step: *Modification of the Structure Model by Rietveld Calculations with NPD Data.* To fit the NPD profile, zero point, background, peak shape functions, and lattice parameters of dehydrated RUB-31 as well as two impurity phases, Li_2SiO_3 and Zn_2SiO_4, were refined. The refined cell parameter of dehydrated RUB-31 $a = 13.6519(2)$ Å is a little bit smaller than as-synthesized RUB-31, 13.6526(1) Å. With the structure model obtained from XPD data analysis, Rietveld calculations began by refining atomic parameters of the oxygen, cesium, and framework T sites. In subsequently calculated Fourier difference maps, two negative peaks were found and assigned to nonframework lithium cation sites Li1 and Li2. The Li1 site is located outside the 6MR windows and with three framework oxygens and one Cs site (Cs3) closer than 2.5 Å, indicative of partial occupancy of both the Cs and Li sites. The Li2 site, off-center from the 8MRs next to 4MR (Figures 1 and 9), is coordinated to four oxygens of 8MR. After refining displacement parameters for all framework tetrahedra, the occupation parameters for framework and nonframework cation sites, including Li1 and Li2,

(18) (a) Liebau, F. *Structural chemistry of silicates*; Springer-Verlag: Berlin, Germany, 1985. (b) Bauer, W. H. *Acta Crystallogr.* **1978**, *B34*, 1751. (c) Renner, B.; Lehmenn., G. *Z. Kristallogr.* **1986**, *175*, 43. (d) Griffen, D. T.; Ribbe, P. H. *Neues Jahrb. Mineral., Abh.* **1979**, *137* (1), 54.

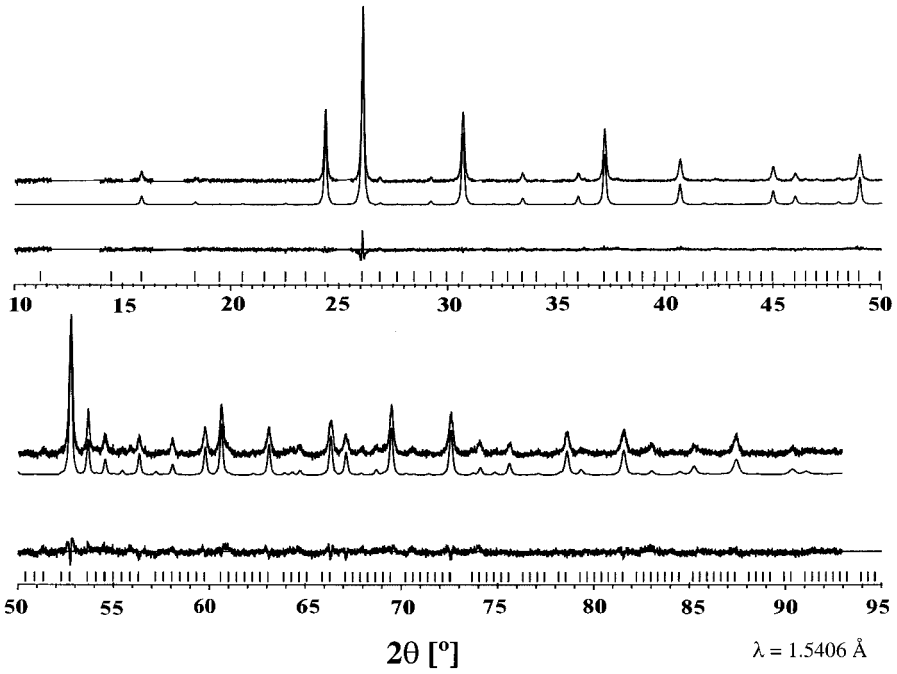

Figure 6. Observed (above) and computed (below) diffraction for the XPD of as-synthesized RUB-31 and the crystallographic model. The lower curve shows the difference between the observed and calculated data. The sets of vertical lines indicate reflections of the material.

Table 3. Atom Coordinates with Standard Deviations in Parenthesis, Isotropic Displacement (U_{iso}), Obtained from Rietveld Refinement with XPD Data[a] of As-Synthesized RUB-31

site	type	*x*	*y*	*z*	U_{iso}
Cs1	Cs	0.1277(3)	0.1277(3)	0.1277(3)	0.0253(3)
Cs2	Cs	0.875	0.875	0.875	0.0253(3)
Cs3	Cs	0.375	0.375	0.375	0.0253(3)
O1	O	0.4049(9)	0.126(1)	0.2824(6)	0.02
O12	O	0.886(1)	0.648(1)	0.7681(5)	0.02
O2	O	0.2167(5)	0.l20(1)	0.367(1)	0.02
O22	O	0.7103(9)	0.5818(9)	0.866(1)	0.02
T1	Si + Zn	0.3377(5)	0.0868(5)	0.3820(5)	0.012(2)
T2	Si	0.125	0.1685(6)	0.41847	0.012(2)
T22	Si + Li	0.625	0.6534(5)	0.90354	0.012(2)

[a] Geometric restraints applied in the final Rietveld calculation: d(T1−O) = 1.75(1) Å, d(T2−O) = 1.60(1) Å, d(T22−O) = 1.63(1) Å, ∠(O−T1−O) = 109(2)°, ∠(O−T2−O) = 109(2)°, ∠(O−T22−O) = 109(2)°, ∠(T1−O1−T2) = 145(8)°, ∠(T1−O12−T22) = 130(8)°, ∠(T2−O2−T1) = 145(8)°, and ∠(T1−O22−T22) = 130(8)°. The final Rietveld refinement resulted in discrepancy indices: $R_{exp} = [(N - P)/\Sigma(w_i Y_{io}^2)]^{0.5} = 0.230$; $R_{wp} = [\Sigma w_i(Y_{io} - Y_{ic})^2/\Sigma w_i Y_{io}^2]^{0.5} = 0.154$; $R_F = \Sigma|I_{hkl,o} - I_{hkl,c}|/\Sigma I_{hkl,o} = 0.134$, where N is number of observations and P is the number of variable parameters.

Table 4. Final Refined Parameters for RUB-31 (Dehydrated at 200 °C) Determined Using the Neutron Powder Data[a]

site	*x*	*y*	*z*	*M*	occupancy	U_{iso}
T1(Si)	0.337(1)	0.089(1)	0.382(1)	24	0.67(6)	0.012(2)
T1(Zn)	0.337(1)	0.089(1)	0.382(1)	24	0.33(5)	0.012(2)
T2(Si)	0.125	0.169(1)	0.419(1)	12	0.95(3)	0.019(4)
T22(Si)	0.625	0.654(1)	0.904(1)	12	0.80(2)	0.011(6)
T22(Li)	0.625	0.654(1)	0.904(1)	12	0.20(2)	0.011(6)
O1(O)	0.404(1)	0.123(1)	0.283(1)	24	1	0.051(5)
O12(O)	0.887(1)	0.645(1)	0.771(1)	24	1	0.053(4)
O2(O)	0.218(1)	0.120(1)	0.364(1)	24	1	0.062(4)
O22(O)	0.711(1)	0.586(1)	0.863(1)	24	1	0.050(5)
Cs1(Cs)	0.129(1)	0.129(1)	0.129(1)	8	0.95(4)	0.03(1)
Cs2(Cs)	0.875	0.875	0.875	4	0.61(6)	0.08(2)
Cs3(Cs)	0.375	0.375	0.375	4	0.58(6)	0.08(2)
Li1(Li)	0.269(5)	0.269(5)	0.269(5)	8	0.4(1)	0.025
Li2(Li)	−0.005(3)	0.004(7)	0.243(6)	24	0.4(1)	0.025

[a] Space group $P4_132$ (Laue symmetry, $m3m$); multiplicity (M) of a general site is 24. The final Rietveld-refinement resulted in discrepancy indices without geometrical restrains: $wR_p = 0.038$, $R_p = 0.031$, $R(F^2) = 0.043$, and $\chi^2 = 1.2$ [$wR_p = (M/\Sigma w I_o^2)^{0.5}$ with $M = \Sigma w(I_o - I_c)^2$; $R_p = \Sigma|I_o - I_c|/\Sigma I_o$; $R(F^2) = \Sigma|F_o^2 - SF_c^2|/\Sigma|F_o^2|$ with S = scale factor; $\chi^2 = M/(N - P)$, where N is the number of observations, and P the number of variable parameters.

were refined at the same time with two constraints. Displacement parameters for sites occupied by cesium were constrained to 0.025 Å^2, the value obtained from the XPD analysis. Constraints consistent with the chemical analysis and analysis of the X-ray data were placed on the occupancies (Occ) of the T sites (i.e., Occ(T1) = Occ(Si) + Occ(Zn), Occ(T2) = Occ(Si), and Occ(T22) = Occ(Si) + Occ(Li)). With these constraints in place, and assuming the oxygen sites were fully occupied, occupancies for the Cs and framework T sites could be refined simultaneously.

The final refinement result (Table 4) clearly showed a partial occupancy of cesium cations on the Cs2 and Cs3 sites, where water molecules may have disordered with Cs cations in the as-synthesized material. As mentioned previously, the Li1 site is 2.5 Å from the Cs3 site, implying the summed occupancies of the two sites does not exceed unity, and the total refined occupancy of these sites is indeed close to this value (Table 4). It is likely the Cs3 site is statistically occupied by Cs cations and water molecules coordinated with non-framework lithium cations in its hydrated form. Because the total number of Cs cations on the Cs sites Cs1, Cs2, and Cs3 (Table 4) is 12 within one unit cell, we estimate that four disordered water molecules occupy this site in as-synthesized RUB-31. As a result, the ratio of Cs to water is 12:4 = 3:1. The chemical analysis value for the ratio of Cs to H_2O was about 2:1. The overestimated total water content for the wet sample may be due to

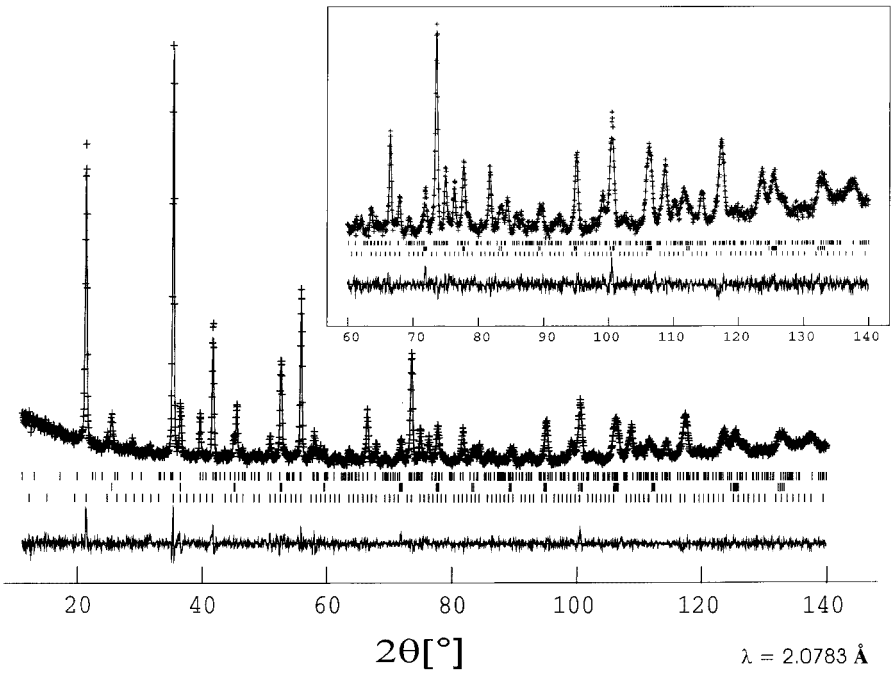

Figure 7. Computed (line) and observed (crosses) diffraction for NPD data of dehydrated RUB-31. The upper, middle, and lower sets of short vertical lines indicate reflections of the impurities (Li_2SiO_3 and Zn_2SiO_4) and RUB-31, respectively. The lower curve shows the difference between the observed and calculated data. The plot is enlarged in the high range angle $60° < 2\theta < 140°$ to emphasize the verified structure model of the new framework material.

the presence of surface water on large crystal surface of extreme small RUB-31 crystals (Graph 1). The ratio of Cs to water (3:1) was also observed in a tetragonal sodium-pollucite ($Cs_{0.7} \sim 0.8Na_{0.1}[Al_{0.8}Si_{2.2}O_6]\cdot(0.3 \sim 0.2)H_2O$).[19] In the case of lithium cations, more than one-third of each of Li1 and Li2 sites are occupied (Table 4), which gives rise to 13 nonframework lithium cations per unit cell of RUB-31.

The refined Zn and Si occupations on the T1 and T2 sites are consistent with the XPD analysis results. The number of Li cations occupying the T22 site estimated from NPD, however, is less than that obtained from chemical analysis and XPD data. This discrepancy may be related to the low sensibility of X-rays for lithium. The former is consistent with a structural formula $Cs_{12}Li_{13}[Li_3Zn_8Si_{37}O_{96}]$ for dehydrated RUB-31. Considering partial occupation of Cs cations on Cs2 and Cs3 sites in dehydrated RUB-31, we suggest an idealized structure formula $Cs_{12}Li_{13}[Li_3Zn_8Si_{37}O_{96}]\cdot 4H_2O$ for hydrated RUB-31. The unit cell content modeled using the NPD data exactly charge-balances the anionic framework and cationic nonframework constituents and confirms the configuration of partially ordered framework tetrahedra T1(Zn,Si), T2(Si), T22(Li,Si) suggested by the XPD analysis.

The final stages of Rietveld analysis using the NPD data included refinements of the displacement parameters for Cs sites, and results are summarized in Table 4 and graphically presented in Figure 7. Selected interatomic distances for framework and nonframework constituents are summarized in Tables 5 and 6, respectively.

Table 5. Selected Interatomic Distances between Framework Cation T and Oxygen *d*(T−O), Their Average Values d_m(T−O), Bonding Angles ∠(O−T−O), and ∠ (T−O−T) within the RUB-31 Structure

d(T−O)	length (Å)	d_m(T−O)	length (Å)	∠(O−T−O)	angle (deg)
T1−O1	1.70(2)			O1−T1−O12	106(1)
T1−O12	1.68(2)			O1−T1−O2	109(1)
T1−O2	1.71(2)			O12−T1−O2	118(1)
T1−O22	1.74(2)	d_m(T1−O)	1.71(2)	O12−T1−O12	112(1)
				O22−T1−O1	109(1)
				O22−T1−O2	104(1)
T2−O1	1.57(2)			O1−T2−O1	105(2)
T2−O1	1.57(2)			O1−T2−O2	111(1)
T2−O2	1.61(2)			O1−T2−O2	113(1)
T2−O2	1.61(2)	d_m(T2−O)	1.59(2)	O1−T2−O2	113(1)
				O1−T2−O2	111(1)
				O2−T2−O2	103(2)
T22−O12	1.63(2)			O12−T22−O12	108(2)
T22−O12	1.63(2)			O12−T22−O22	113(1)
T22−O22	1.61(2)			O12−T22−O22	113(1)
T22−O22	1.61(2)	d_m(T22−O)	1.62(2)	O12−T22−O22	112(1)
				O12−T22−O22	112(1)
				O22−T22−O22	98(1)
				∠(T−O−T)	angle (deg)
				T1−O1−T2	148(1)
				T1−O12−T22	139(1)
				T1−O2−T2	142(1)
				T1−O22−T22	136(1)

Structure Description. RUB-31, $(Cs_{12}Li_{13}[Li_3Zn_8Si_{37}O_{96}])\cdot 4H_2O$, consists of a three-dimensioal network of $[LiO_4]$, $[ZnO_4]$,and $[SiO_4]$ tetrahedra. These are statically disordered on three symmetrically unique tetrahedral sites. However, framework Zn cations are distributed exclusively on the T1 site, while framework Li are present only on the T22 site, and the T2 site is occupied only by Si. $[T1O_4]$, $[T2O_4]$, and $[T22O_4]$ tetrahedra are connected to build a chainlike partial struc-

(19) Frank-Kamenetskaya, O. V.; Rozhdestvenskaya, I. V.; Bannova, I. I.; Kostitsyna, A. V.; Kaminskaya, T. N.; Gordienko, V. V. *Transl. Kristallogr.* **1995**, *40* (4), 698.

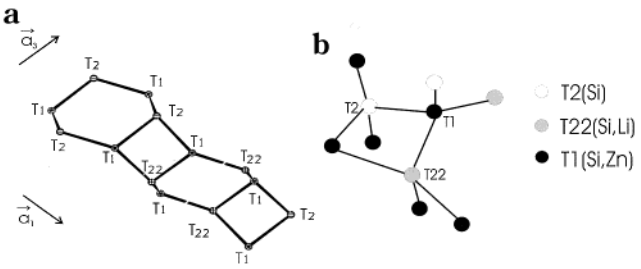

Figure 8. (a) Arrangement of [T1O$_4$], [T2O$_4$], and [T22O$_4$] tetrahedra in a sequence of 6MR(I)−4MR−6MR(II) of the RUB-31 framework. Oxygen atoms are omitted for clarity. (b) Neighborhood of framework cation sites T1, T2, and T22.

Table 6. Selected Interatomic Distances between Nonframework Cesium and Lithium and Nearest-Neighbor Oxygen in the Dehydrated RUB-31 Structure Based on the Results from NPD Data Analysis

d(Cs−O)	length (Å)	*d*(Li−O)	length (Å)
3*x* Cs1−O2	3.45(2)	3*x* Li1−O2	2.51(4)
3*x* Cs1−O2	3.56(2)	3*x* Li1−O1	2.72(1)
3*x* Cs1−O22	3.12(1)	Li1−Cs3	2.5(1)
3*x* Cs1−O22	3.57(2)		
		Li2−O22	2.02(8)
6*x* Cs2−O1	3.26(1)	Li2−O22	2.17(9)
6*x* Cs2−O12	3.46(2)	Li2−O2	2.35(8)
		Li2−O2	2.53(8)
6*x* Cs3−O1	3.67(2)	Li2−O12	2.63(6)
6*x* Cs3−O12	3.58(2)	Li2−O1	2.73(6)

Table 7. Possible Si Neighboring on Each T1, T2, and T22 Site in the Framework of RUB-31 and Corresponding Q^4 Unit[a]

possible atom type of four direct neighbor T sites				type of Q^4 unit
T2	T2	T22	T22	
		Si on T1		
Si (1)[b]	Si (1)	Si (4/5)	Si (4/5)	Q^4[4Si]
Si (1)	Si (1)	Si (4/5)	Li (1/5)	Q^4[3Si 1Li]
Si (1)	Si (1)	Li (1/5)	Li (1/5)	Q^4[2Si 2Li]
T1	T1	T1	T1	type of Q^4 unit
		Si on T2		
Si (2/3)	Si (2/3)	Si (2/3)	Si (2/3)	Q^4[4Si]
Si (2/3)	Si (2/3)	Si (2/3)	Zn (1/3)	Q^4[3Si 1Zn]
Si (2/3)	Si (2/3)	Zn (1/3)	Zn (1/3)	Q^4[2Si 2Zn]
Si (2/3)	Zn (1/3)	Zn (1/3)	Zn (1/3)	Q^4[1Si 3Li]
Zn (1/3)	Zn (1/3)	Zn (1/3)	Zn (1/3)	Q^4[0Si 4Zn]
T1	T1	T1	T1	type of Q^4 unit
		Si on T22		
Si (2/3)	Si (2/3)	Si (2/3)	Si (2/3)	Q^4[4Si]
Si (2/3)	Si (2/3)	Si (2/3)	Zn (1/3)	Q^4[3Si 1Zn]
Si (2/3)	Si (2/3)	Zn (1/3)	Zn (1/3)	Q^4[2Si 2Zn]
Si (2/3)	Zn (1/3)	Zn (1/3)	Zn (1/3)	Q^4[1Si 3Zn]
Zn (1/3)	Zn (1/3)	Zn (1/3)	Zn (1/3)	Q^4[0Si 4Zn]

[a] Among them, Q^4[4Si], and Q^4[3Si 1Zn], and Q^4[3Si 1Li] units might most frequently reveal to the partially disordered RUB-31 framework structure, based on occupancy values of their tetrahedral atoms. [b] Occupancy of the atom type on each T site.

ture consisting of one 4MR and two 6MRs, 6MR(I) and 6MR(II), with a sequence of 6MR(I)−4MR−6MR(II) (Figure 1). The arrangement of T1, T2, and T22 within this partial structure is as follows (Figure 8a): 6MR(I), T1-T2-T1-T2-T1-T2; 4MR, T1-T2-T1-T22; 6MR(II), T1-T22-T1-T22-T1-T22.

In this geometry, each [T1O$_4$] tetrahedron is directly connected to two [T2O$_4$] tetrahedra and two [T22O$_4$] tetrahedra while all [T2O$_4$] and [T22O$_4$] tetrahedra are directly bonded to only four [T1O$_4$] tetrahedra (Figure 8b). This is very like the Al avoidance in aluminosilicate framework structures,[20] distributing the more highly negatively charged $(ZnO_2)^{2-}$ and $(LiO_2)^{3-}$ as far apart as possible by always making sure there is a neutral-charged (SiO_2) moiety in between.

The ^{29}Si MAS NMR resonance resolved into three peaks (Figure 2) is also consistent with the configuration of T site occupancies. As given in Table 7, all possible types for the direct neighbors of Si on each T1, T2, and T22 site are of interest in ^{29}Si NMR spectra of the disordered RUB-31 framework. Silicon on T1 has three possible different neighborhoods, while silicon on T2 and T22 have five. Principally, all of these short-range order around each Si, as described with Q^4[*n*Si(4 − *n*)T] (*n* = 4 ∼ 0; T = Li or Zn),[21] contributed to the intensity of the ^{29}Si MAS NMR spectrum. On the basis of occupancy values of Si, Li, and Zn on T1, T2, and T22 sites, the Q^4[4Si] arrangement should appear most common and then Q^4[3Si1Zn] to be followed by Q^4[3Si1Li] (Table 7). These three types Q^4[4Si], Q^4[3Si1Zn], and Q^4[3Si1Li] for Si neighboring should contribute relatively more to peak intensity than the other Q^4 units, and their resonance positions might be shifted from each other. This can be seen in the obtained fine structure of the ^{29}Si MAS NMR resonance, and their chemical shifts are consistent with the assignment of Q^4[4Si], Q^4[3Si1Zn], and Q^4[3Si1Li] in ^{29}Si MAS NMR spectra of known litho- and zincosilicate materials.[10,11,16]

The mean value of bonding distances within the RUB-31 framework structure, d_m(T1−O) = 1.71 Å, d_m(T2−O) = 1.59 Å, d_m(T22−O) = 1.62 Å, are compared to those in known Al-, Be-, Mg-bearing pollucite in Table 8. It is clear from this analysis that mean values of bonding distances d_m(T−O) are mainly dependent on the type and amount of substituting atoms disordered with silicon on each T sites. The bonding distances within disordered framework tetrahedra T1(Zn,Si) and T22-(Li,Si) are also narrowly correlated with the amounts of Zn and Li on the sites.

In the pore system of RUB-31 (Figure 9), the Cs1 site is occupied by eight Cs cations while each of the other sites, Cs2 and Cs3, contains two Cs cations and two water molecules. In the ^{133}Cs MAS NMR spectrum of as-synthesized RUB-31 (Figure 3), the intensity ratio of the resonance at 5 ppm to that at 63 ppm is 2:1. From this observation, the resonance at 5 ppm may be due to Cs cations on the Cs1 site and another resonance at 63 ppm due to Cs2 and Cs3.

Eleven nonframework Li cations are statically disordered in two different sites Li1 and Li2 (Figure 9). The Li1 site is present in windows of 6MRs. The water molecules on Cs3 may be also considered as a nearest coordination species for Li1. The Li2 site is located within in 8MRs connected to 4MRs and bounded with six oxygen atoms of 8MR and 4MR in varying distances between 2.0 and 2.7 Å (Table 6). Unfortunately, ^{7}Li MAS NMR could not differentiate three different sites of lithium, Li1, Li2, and T22, from each other.

(20) Loewenstein, W. *Am. Mineral.* **1954**, *39*, 92.
(21) (a) Engelhardt, G.; Michel, D. *High-resolution solid-state NMR of silicates and zeolites*; John Wiley and Sons: New York, 1987. (b) Kato, M.; Hattori, T. *Phys. Chem. Miner.* **1998**, *25*, 556.

Table 8. Comparison of Mean Bonding Distances in Disordered Pollucite-Type Framework Structures[a]

pollucite and pollucite analogues	type and amount of disordered framework atoms	mean value of bonding distances in disordered framework structure (Å)	mean value of bonding distances for four-coordination observed in silicates (Å)[18]	ionic radius of cations with 4-fold coordination (Å)[26]
$Cs[AlSi_2O_6]$	16Al + 32Si	$d_m(T-O) = 1.643$[1]	$d_m(Al-O) = 1.75$ Å	$r(Al^{3+}) = 0.39$
$Cs[Be_{0.5}Si_{2.5}O_6]$	8Be + 40Si	$d_m(T-O) = 1.606$[25]	$d_m(Be-O) = 1.64$ Å	$r(Be^{2+}) = 0.27$
$Rb[Mg_{0.5}Si_{2.5}O_6]$	8Mg + 40Si	$d_m(T-O) = 1.619$[5]	$d_m(Mg-O) = 1.92$ Å	$r(Mg^{2+}) = 0.57$
RUB-31	T1:8Zn + 16Si	$d_m(T1-O) = 1.71$	$d_m(Zn-O) = 1.96$ Å	$r(Zn^{2+}) = 0.60$
$(Cs_{12}Li_{13}[Li_3Zn_7Si_{38}O_{96}])\cdot 4H_2O$	T22:3Li + 9Si	$d_m(T22-O) = 1.62$	$d_m(Li-O) = 1.96$ Å	$r(Li^{+}) = 0.59$
	T2:12Si	$d_m(T2-O) = 1.59$	$d_m(Si-O) = 1.60$ Å	$r(Si^{4+}) = 0.26$

[a] These values are narrowly correlated with amount and type of framework cations substituting silicon.

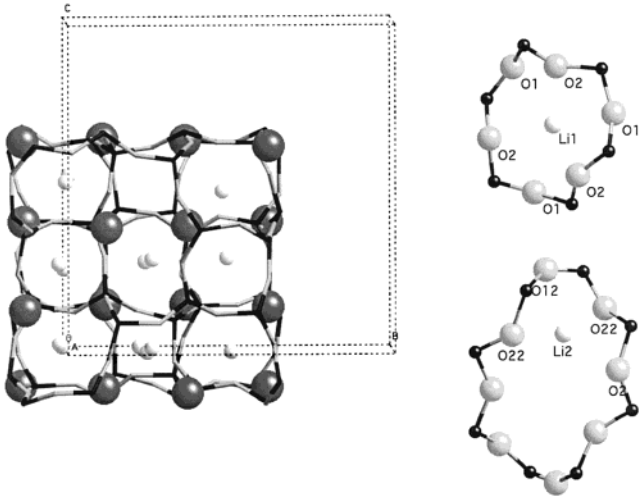

Figure 9. Distribution of 12-coordinate nonframework Cs disordered with water molecules (larger circles) and Li cations in octahedral vacancies (smaller circles) over the RUB-31 pore system. Details of lithium cations sites Li1 and Li2 are presented extra in the right side of the figure.

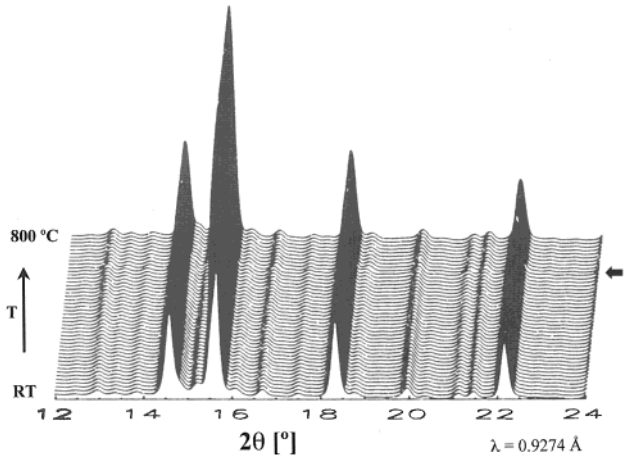

Figure 10. Synchrotron XPD diagrams detected while heating as-synthesized RUB-31 between RT and 800 °C. With increasing temperature up to 800 °C, no discontinuity was observed, except for a light mechanical shift of the detector (marked with a short arrow in the right side of XPD diagrams).

The highest topological symmetry for ANA (pollucite) analogues in which framework T sites are randomly occupied is cubic ($Ia\bar{3}d$). The cell parameter a varies between 13.3 and 13.8 Å, depending upon substitutions in the framework and nonframework sites. Distortions from the ideal $Ia\bar{3}d$ symmetry, to one of its subgroups, occur as a result of ordering in either the framework or no-framework sites. For example, Frank-Kamenetska et al.[19] observed a phase transition from I_1/acd to $Ia\bar{3}d$ in sodium-pollucite ($Cs_{0.7} \sim 0.8Na_{0.1}[Al_{0.8}Si_{2.2}O_6]\cdot(0.3 \sim 0.2)H_2O$) below 50 °C, resulting from a disordering of sodium over the available octahedral sites in the pore system. On the other hand, Mazzi and Galli[22] showed that for Al/Si close to $^1/_2$ a partial ordering of Al over the T sites results in a lowering of symmetry to tetragonal (I_1/acd) or orthorhombic ($Ibca$). Artioli et al.[23] also reported partial T site ordering in $Na_{13}[Al_{24}P_{11}Si_{13}O_{96}]\cdot 16H_2O$. The framework displays an alternation of 24Al and (11P + 13Si) over the T sites, which is directly responsible for the symmetry lowering from the ideal symmetry of analcime, $Ia\bar{3}d$, to I_132. The authors also described a possibility that a ordering of Si and P atoms onto two different sites to change the lattice type from body-centered to primitive (i.e., $I4_132 \rightarrow P4_132$ or $P4_12_12$). Here, the sequence of T atoms of a 6MR−4MR−6MR chain within the framework determines the symmetry: $P4_132$ can be derived with a sequence of (AlSiAlSiAlSi)−(AlSiAlP)−(AlPAlPAlP) while another possible arrangement (AlSiAlSiAlP)−(AlSiAlP)−(AlPAlPAlSi) results in the lower space group symmetry $P4_12_12$. In the case of $Na_{13}[Al_{24}P_{11}Si_{13}O_{96}]\cdot 16H_2O$, a phase transition due to order−disorder over tetrahedral sites can occur only at higher temperatures (300 ∼ 600 °C) in contrast to the case of the phase transition correlated with the statistic distribution over octahedral nonframework sites. Clearly, the space group symmetries of members of the ANA family are affected mainly by order−disorder at framework and nonframework sites rather than being simply a function of chemical compositions. In the present work, we have also demonstrated partially ordered framework atom sites occupied by Li, Zn, and Si, which is related to the dissymmetrization of $Cs_{12}Li_{13}[Li_3Zn_8Si_{37}O_{96}]\cdot 4H_2O$ from body-centered cubic pollucite ($Ia\bar{3}d$) to $P4_132$.

The new structure shows the highest ratio of nonframework cations (M) to substituting T atoms (i.e., with M/T = 2.3:1 among the pollucite family members showing M/T ratio of between 1:1 and 2:1). Furthermore, RUB-31 still contains a high amount of silicon atoms with a ratio of Si/T = 3.4:1. This value varies between 1:1 and 5:1 for known ANA-type materials. Usually, higher Si/T ratios increase the thermal stability of microporous silicate compounds.[24] With the discovery

(22) Mazzi, F.; Galli, E. *Am. Mineral.* **1978**, *63*, 448.
(23) Artioli, G.; Pluth, J. J.; Smith, J. V. *Am. Mineral.* **1984**, *C40*, 214.
(24) Park, S.-H.; Grosse Kunstleve, R.-W.; Graetsch, H.; Gies, H. *Progress in Zeolite and Microporous Materials, Studies in Surface Science and Catalysis 105*; Chon, H., Ihm, S.-K., Uh, Y. S., Eds.; Elsevier Science: New York, 1997; pp 1989−1994.
(25) Torres-Martinez, L. M.; Gard, J. A.; Howie, R. A.; West, A. R. *J. Solid State Chem.* **1984**, *51*, 100.

of RUB-31, it has been demonstrated that lithium can replace silicon in high silica microporous materials. This could allow for a higher number of extra framework cations in a material with a higher thermal stability.

The high thermal stability of RUB-31 was demonstrated in in situ dehydration experiments with RUB-31 between RT and 800 °C (Figure 10). There was no discontinuity while changing temperature and, therefore, no evidence of any phase transitions up to 800 °C. The structure maintains the space group symmetry $P4_1$-32 in this temperature range.

(26) (a) Shannon, R. D.; Prewitt, C. T. *Acta Crystallogr.* **1969**, *B25*, 925. (b) Shannon, R. D. *Acta Crystallogr.* **1976**, *A32*, 759.

Acknowledgment. We acknowledge financial support from the NSF via DMR-0095633. Dr. Jonathan Hanson has our special thanks for support in collecting time-resolved synchrotron X-ray powder data of RUB-31 samples at the beam line X7B at NSLS in Brookhaven National Laboratory. The research at NSLS beam line X7B was supported under Contract DE-AC02-98CH-110886 with the Department of Energy by its Division of Chemical Sciences, Office of Basic Energy Research. We also thank Professor Colin A. Fyfe (Department of Chemistry, University of British Columbia, BC, Canada) for his scientific advice and discussion on ^{29}Si MAS NMR of RUB-31.

CM020226W